Kinetic Control of the Oxidative Coupling of $[B_2H_4Fe_2(CO)_6][Li]_2$. X-ray Crystal Structures and Interconversion of *B,Fe-conjuncto*-$\{B_2H_4Fe_2(CO)_6\}_2$ and *B,B-conjuncto*-$\{B_2H_4Fe_2(CO)_6\}_2$

Chang-Soo Jun,† Douglas R. Powell,‡ Kenneth J. Haller,† and Thomas P. Fehlner*,†

Department of Chemistry and Biochemistry, University of Notre Dame, Notre Dame, Indiana 46556, and Department of Chemistry, University of Wisconsin, Madison, Wisconsin 53706

Received May 20, 1993•

The reaction of $B_2H_6Fe_2(CO)_6$ with *t*-BuLi yields $[B_2H_4Fe_2(CO)_6][Li]_2$. The reaction of this dilithio salt with $FeCl_2$ followed by $FeCl_3$ at low temperature leads to the formation of *B,Fe-conjuncto*-$\{B_2H_4Fe_2(CO)_6\}_2$, **I**, in 40% yield. Heating leads to the formation of an equilibrium mixture of **I** and *B,B-conjuncto*-$\{B_2H_4Fe_2(CO)_6\}_2$, **II**, with $K = [II]/[I] \approx 2$. Both **I** and **II** have been characterized in the solid state by single-crystal X-ray diffraction studies (**I**,orthorhombic, *Pbca* (No. 61), $a = 12.990(4)$ Å, $b = 12.279(3)$ Å, $c = 26.527(10)$ Å, $V = 4231.2$ Å^3, d(calcd) = 1.92 g/cm^3, $Z = 8$; **II**,monoclinic, $P2_1$, $a = 7.3740(10)$ Å, $b = 13.956(3)$ Å, $c = 10.627(2)$ Å, $\beta = 106.22(3)°$, $V = 1050.1(3)$ Å^3, d(calcd) = 1.932 g/cm^3, $Z = 2$) as well as spectroscopically in solution. Although the structural form of **I** is the same in the solid state and solution, **II** exists in three tautomeric forms in solution the most abundant of which (**IIa**) corresponds to the form found in the solid state. Postulated structures for the other two tautomers of **II** are presented. While **I** shows no evidence of fluxional behavior in the solution ^{1}H NMR spectrum, **IIa** does. The equilibrium mixture of **I** and **II** can be prepared in very low yield by the direct pyrolysis of $B_2H_6Fe_2(CO)_6$ corroborating the fact that oxidative coupling of the dianion produces a kinetic product.

The oxidation of anionic transition metal clusters is an established, if not fully understood, method for effecting a number of chemical transformations. For example, in the absence of cluster rearrangement, the two-electron oxidation of a cluster dianion produces a neutral unsaturated cluster which can pick up a two-electron donor. Hence, oxidation provides a route for the introduction of a two-electron donor into a cluster under mild conditions.[1-4] However, the oxidation of anionic clusters can also lead to both increases and decreases in cluster nuclearity.[5-7] One might view the former as arising from the addition of a metal fragment rather than a simple ligand. In the case of borane and carborane cluster chemistry, oxidative coupling has already been developed as a useful synthetic method by Grimes and co-workers.[8,9] It is of particular interest to note that the mild reaction conditions foster the isolation of kinetic products. Here we present a related approach to the systematic construction of larger metallaborane clusters from metallaborane cluster dianion building blocks. This constitutes a new cluster building method in the metallaborane area.[10-12]

In a preliminary communication[13] we described the isolation of *conjuncto*-$[B_2H_4Fe_2(CO)_6]_2$ (**I**) formed from the reaction of $[B_2H_4Fe_2(CO)_6][Li]_2$ with $(CO)_4FeBr_2$. The reaction is formally oxidative coupling; however, the low yield of the coupled product combined with the large variety of other products prevented any firm conclusions concerning the reaction type. In the following, we demonstrate that **I** does indeed arise from an oxidative coupling reaction of the dianion and, relative to the thermal coupling of $B_2H_6Fe_2(CO)_6$, **I** is a kinetic product that can be equilibrated with a somewhat more stable isomeric form.

Chart I

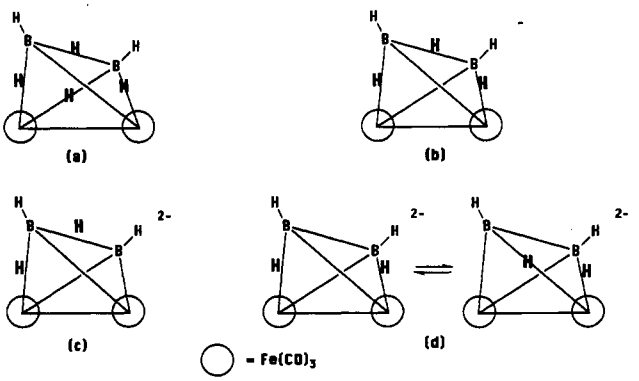

Results

$[B_2H_4Fe_2(CO)_6][Li]_2$. In spite of the fact that cleavage of THF by butyllithium takes place at higher temperatures, the reaction of butyllithium with $B_2H_6Fe_2(CO)_6$ in THF smoothly forms the mono- and then the dilithio-salt (70% yield by IR or ^{11}B NMR) at low temperature. The second equivalent of butyllithium must be added very slowly, and excess reagent must be avoided. The lithium salt of the dianion can be isolated as a crystalline material from THF and has been characterized spectroscopically. The variable temperature ^{1}H spectra show that it is present as two tautomeric forms in solution having the probable structures shown in Chart Id. The dianion is usually prepared and used *in situ*.

The IR spectra of $B_2H_6Fe_2(CO)_6$ and the two anions derived from it are shown in Figure 1. The ≈50 cm^{-1} incremental shift to lower energy of the CO stretching bands on deprotonation is consistent with the sequential loss of two protons. The two BH

† University of Notre Dame.
‡ University of Wisconsin.
• Abstract published in *Advance ACS Abstracts*, October 1, 1993.

(1) Simerly, S. W.; Wilson, S. R.; Shapley, J. R. *Inorg. Chem.* **1992**, *31*, 5146.
(2) Drake, S. R.; Johnson, B. F. G.; Lewis, J.; Conole, G.; McPartlin, M. *J. Chem. Soc., Dalton Trans.* **1990**, 995.
(3) Beringhelli, T.; D'Alfonso, G.; De Angelis, M.; Ciani, G.; Sironi, A. *J. Organomet. Chem.* **1987**, *322*, C21.
(4) Ceriotti, A.; Della Pergola, R.; Demartin, F.; Garlaschelli, L.; Manassero, M.; Masciocchi, N. *Organometallics* **1992**, *11*, 756.
(5) Della Pergola, R.; Demartin, F.; Garlaschelli, L.; Manassero, M.; Martinengo, S.; Sansoni, M. *Inorg. Chem.* **1987**, *26*, 3487.
(6) Beringhelli, T.; D'Alfonso, G.; Molinari, H.; Sironi, A. *J. Chem. Soc., Dalton Trans.* **1992**, 689.
(7) Hsu, G.; Wilson, S. R.; Shapley, J. R. *Inorg. Chem.* **1991**, *30*, 3881.
(8) Grimes, R. N. *Carbon-Rich Carboranes and Their Metal Derivatives*; American Chemical Society: Washington, DC, 1983; Vol. 26, p 55.
(9) Grimes, R. N. In *Inorganometallic Chemistry*; Fehlner, T. P., Ed.; Plenum: New York, 1992; p 253.
(10) Kennedy, J. D. *Prog. Inorg. Chem.* **1986**, *34*, 211.
(11) Kennedy, J. D. *Prog. Inorg. Chem.* **1984**, *32*, 519.
(12) Housecroft, C. E.; Fehlner, T. P. *Adv. Organomet. Chem.* **1982**, *21*, 57.
(13) Jun, C.-S.; Meng, X.; Haller, K. J.; Fehlner, T. P. *J. Am. Chem. Soc.* **1991**, *113*, 3603.

0020-1669/93/1332-5071$04.00/0

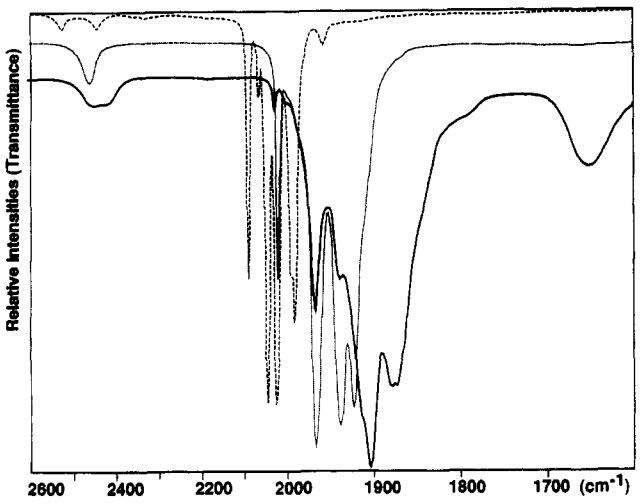

Figure 1. IR spectra in the BH and CO stretching regions of $B_2H_6Fe_2(CO)_6$ (dashed line), $[B_2H_5Fe_2(CO)_6][Li]$ (dotted line), and $[B_2H_4Fe_2(CO)_6][Li]_2$ (solid line).

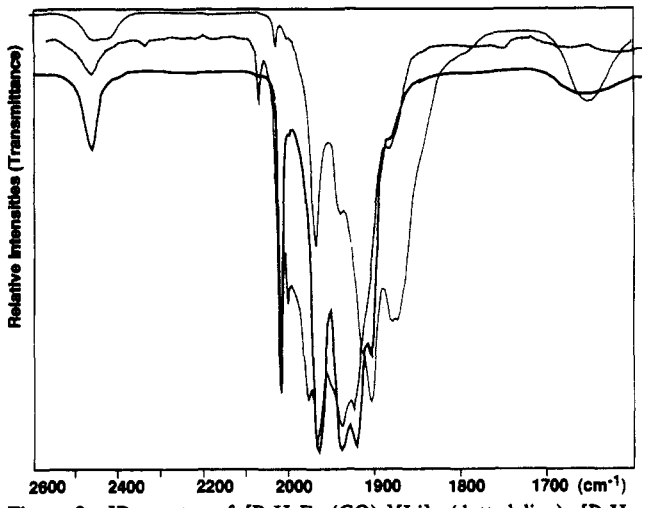

Figure 2. IR spectra of $[B_2H_4Fe_2(CO)_6][Li]_2$ (dotted line), $[B_2H_4Fe_2(CO)_6][Li]_2 + {}^1/_2FeCl_2$ (solid line), and $[B_2H_4Fe_2(CO)_6][Li]_2 + {}^1/_2FeCl_2 + FeCl_3$ (dashed line).

stretching vibrations observed for $B_2H_6Fe_2(CO)_6$ ($\Delta\nu = 82$ cm^{-1}) are consistent with its asymmetric static structure (Chart Ia).[14] This proposed structure has been corroborated by the X-ray crystal structure of an analogous tantalum derivative[15] as well as by that of the dimer discussed below. The monoanion shows a single BH stretch consistent with a postulated structure possessing vibrationally uncoupled, equivalent BH fragments (Chart Ib).[14] The dianion shows two BH stretches ($\Delta\nu = 29$ cm^{-1}) which is consistent with either inequivalent BH fragments (Chart Ic) or coupling of equivalent BH vibrations through the cage network (Chart Id).

In contrast to the neutral molecule and monoanion, the proton NMR of the dianion at room temperature exhibits a broad resonance at δ −5.2 which is consistent with averaged BH (and BHB) and BHFe resonances. At lower temperatures only a resonance at −11.5 is observed and its partner(s) is (are) presumed hidden by the strong and somewhat broadened resonances of the THF coming from that coordinated to Li^+ as well as the solvent (calcd position δ 1.09 for a structure with two BH and BHFe protons). At −90 °C the resonance at −11.5 splits into two and a shoulder is observed at 0.6. These incomplete data suggest Id as the structure of the dianion with the two tautomeric forms shown existing in solution. This is a bit surprising in that the isoelectronic cobaltaborane, $B_2H_4Co_2(CO)_6$, clearly has structure Ic[16] and empirically we know that BHFe hydrogens are more protonic than BHB protons. However, there are two additional factors to consider. First, the IR spectrum suggests the presence of one, perhaps two, bridging carbonyls. Second, it may well be that one Li^+ is very strongly coordinated on the B–B edge thereby favoring structures Id. Note that as the hydrogens on the dianion are observed to be fluxional, the difference in energies of the possible tautomeric structures must be small and the most stable locations of the cluster hydrogens should be of little consequence in terms of reactivity.

***B,Fe-conjuncto*-$\{B_2H_4Fe_2(CO)_6\}_2$ (I).** This compound is prepared in good yield from $[B_2H_4Fe_2(CO)_6]^{2-}$ according to reactions 1 and 2.

$$2[B_2H_4Fe_2(CO)_6][Li]_2 + FeCl_2 \rightarrow [\{B_2H_4Fe_2(CO)_6\}_2Fe][Li]_2 + 2LiCl \quad (1)$$

$$[\{B_2H_4Fe_2(CO)_6\}_2Fe][Li]_2 + 4FeCl_3 \rightarrow \{B_2H_4Fe_2(CO)_6\}_2 + 5FeCl_2 + 2LiCl \quad (2)$$

The evidence for this set of reactions is as follows. Excess $FeCl_2$ enhances the reaction yield somewhat, but the stoichiometry with respect to $FeCl_3$ is critical. As expected, this is consistent with a role of Fe(II) in coordination of the dianion and Fe(III) as the oxidizing agent. The coupled product, $\{B_2H_4Fe_2(CO)_6\}_2$ (I), is not formed from $[B_2H_4Fe_2(CO)_6]^{2-}$ with either $FeCl_2$ or $FeCl_3$ alone. Oxidation with $[Cp_2Fe]^+$ or Ag(I) (or $FeCl_3$ alone) leads to degradation of the reactant dianion with no evidence for the formation of I. Nor is coupling observed when the monoanion, $[B_2H_5Fe_2(CO)_6]^-$, is subjected to the same reaction conditions as the dianion.

A modestly stable intermediate has been observed by IR spectroscopy. Figure 2 shows significant changes in the carbonyl stretching region on the addition of ${}^1/_2$ equiv of $FeCl_2$ to the dianion. The absorption pattern is similar but not the same as that for $[B_2H_5Fe_2(CO)_6]^-$. An important difference is the fact that six bands are observed showing that the pseudo C_{2v} symmetry of the monomers is effectively broken. In this sense, the IR spectrum is similar to that of the coupled product (see below). This leads us to formulate the intermediate as a coordination complex between Fe(II) and two dianion ligands; i.e., with an overall charge of −2 on the intermediate, each ferraborane is effectively monoanionic consistent with the energy range of the CO absorptions. Also shown in Figure 2 is the result of the addition of ${}^1/_2$ equiv of $FeCl_2$ and 1 equiv of $FeCl_3$ to the dianion. The spectrum is now more complex. The oxidation reaction appears to be slow, and while the intermediate is still evident, neither of the primary final separated products, $B_2H_6Fe_2(CO)_6$ and $\{B_2H_4Fe_2(CO)_6\}_2$, is evident. The presence of the former product suggests that an adventitious source of protons (or hydrogen atoms) is present. Both of these compounds are subject to deprotonation in THF solution, and as the bands attributed to the intermediate are very similar to those of $[B_2H_5Fe_2(CO)_6]^-$, the presence of $[B_2H_5Fe_2(CO)_6]^-$ cannot be completely ruled out. However, it is clear that $[\{B_2H_4Fe_2(CO)_6\}_2]^-$ is not present (absence of a band at 2066 cm^{-1}). The new bands are attributed to a second intermediate, $[\{B_2H_4Fe_2(CO)_6\}_2Fe]^-$, from the one-electron oxidation of the first intermediate.

Although the basic structural data on the principal product of the oxidative coupling of $[B_2H_4Fe_2(CO)_6]^{2-}$, $\{B_2H_4Fe_2(CO)_6\}_2$ (I), has been communicated previously,[13] a number of points are elaborated in order to provide an appreciation of the nature of the isomerization reaction reported below. First, the IR spectrum (Figure 3), although reminiscent of that of $B_2H_6Fe_2(CO)_6$, is significantly different from the expected spectrum for an $X_2M_2(CO)_6$ complex with C_{2v} symmetry.[17] The strong band at 2073 cm^{-1} is particularly noteworthy in that there is no corresponding

(14) Jacobsen, G. B.; Andersen, E. L.; Housecroft, C. E.; Hong, F.-E.; Buhl, M. L.; Long, G. J.; Fehlner, T. P. *Inorg. Chem.* **1987**, *26*, 4040.
(15) Ting, C.; Messerle, L. *J. Am. Chem. Soc.* **1989**, *111*, 3449.
(16) Jun, C.-S. Ph.D Thesis, University of Notre Dame, 1993.
(17) Bor, G. *J. Organomet. Chem.* **1975**, *94*, 181.

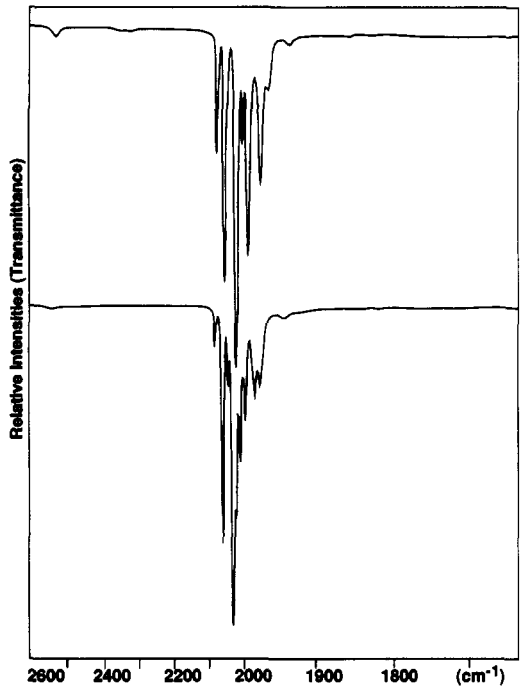

Figure 3. IR spectra of *B,Fe-conjuncto*-$\{B_2H_4Fe_2(CO)_6\}_2$ (I) (top) and *B,B-conjuncto*-$\{B_2H_4Fe_2(CO)_6\}_2$ (II) (bottom).

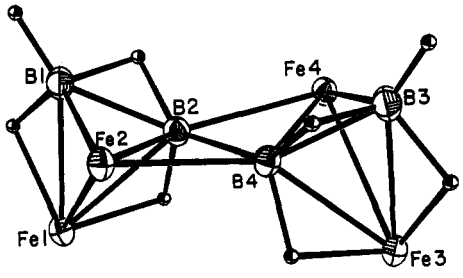

Figure 4. Structure of *B,Fe-conjuncto*-$[B_2H_4Fe_2(CO)_6]_2$ (I)in the solid state. The hydrogen atoms were located and refined. The three terminal CO ligands on each Fe atom are not shown for clarity.

band in $B_2H_6Fe_2(CO)_6$. Second, the solution ^{11}B and ^1H NMR data are consistent with the solid-state structure (Figure 4), which consists of two tetrahedral B_2Fe_2 cages related by a C_2 axis joined along an Fe–B edge of each such that the four bridgehead atoms define a butterfly structure. That is, there are two equivalent BH and B fragments, two pairs of equivalent BHFe and two equivalent BHB bridging hydrogens. The ^1H NMR is invariant from −90 to 50 °C. Above this temperature isomerization to **II** begins (see below). Note that in the same temperature regime, $B_2H_6Fe_2(CO)_6$ exhibits a complex fluxional behavior involving all the hydrogen atoms in the molecule.[14] Third, as expected, the Fe–B distances associated with the B–H–Fe interactions (2.194(2) Å) lie in the range for open three-center interactions similar to those observed in $B_3H_7Fe_2(CO)_6$.[18]

***B,B-conjuncto*-$\{B_2H_4Fe_2(CO)_6\}_2$ (II).** As the molecular formula of I, $B_4H_8Fe_2(CO)_{12}$, is also consistent with a single open cage structure,[19,20] we investigated its thermal isomerization. Heating a sample of pure I to 80–90 °C for 1 h or longer resulted in the complex ^{11}B NMR spectrum illustrated at the top of Figure 5. Initially we thought that we had to deal with a reaction mixture; however, chromatography yielded only two products one of which was I. The other produced the ^{11}B NMR spectrum shown at the bottom of Figure 5, where it can be seen that all the resonances in the reaction mixture not due to I appear. The six resonances and the odd intensities suggest the presence of more than one

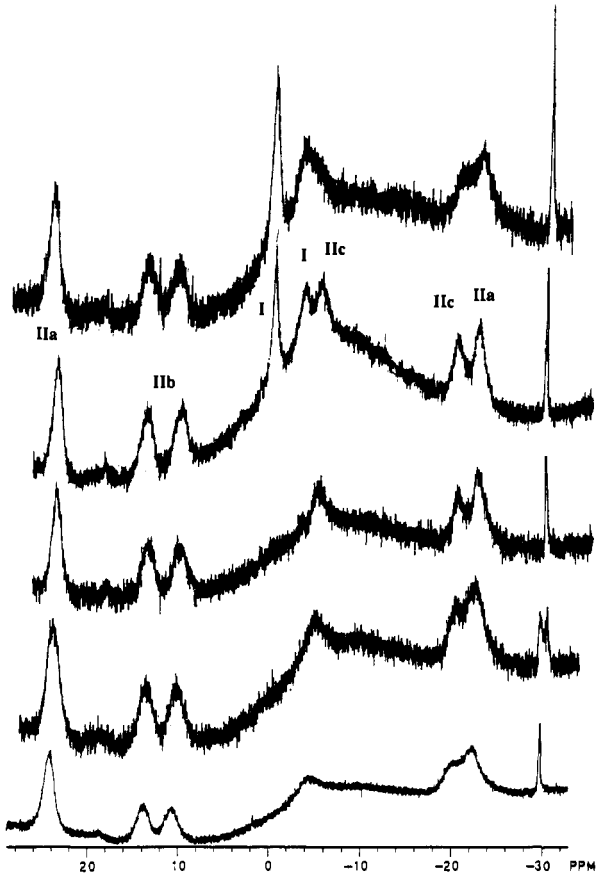

Figure 5. ^{11}B NMR spectra of *B,B-conjuncto*-$\{B_2H_4Fe_2(CO)_6\}_2$ (II) as a function of temperature. Key (from the bottom): 20 °C, 50 °C, 70 °C, 80 °C, return to 20 °C. The topmost spectrum, which is that of an equilibrium mixture of *B,Fe-conjuncto*-$[B_2H_4Fe_2(CO)_6]_2$, I, and II, is identical to one obtained by heating a pure sample of I. The broad powder signal is caused by boron in the NMR probe.

species. The IR spectrum of the chromatographed material is a little more complex than that of I but not sufficiently so to suggest a mixture of clusters of differing nuclearities. These observations, plus the fact that the mass spectrometric experiments showed a single molecular type having a molecular formula $B_4H_8Fe_4(CO)_{12}$, suggest an equilibrium mixture of tautomeric forms of a geometric isomer of I. Although this introduces additional complexity into the problem of characterization, it can no longer be considered an unusual situation in cluster systems.[21–23]

Single crystals were isolated from the solution containing II. The structure of the tautomer trapped in the solid state is shown in Figure 7, where it may be seen that **IIa** has a geometric structure very similar to that of I. The difference is that the intercage connection arises from the interaction of two boron atoms on each cage rather than a boron and iron atom each. Other than this important difference in connectivity, the structural parameters of the two isomers are very similar.

The ^{11}B NMR as a function of time after dissolving crystals of II shows the same number of resonances but with the intensities of two of the features enhanced (Figure 6). Over a period of time the intensities change until the typical equilibrium ratio is once more achieved. This observation allows the signals at δ 24.2 and −21.9 to be identified with the form observed in the solid state. The two other pairs of signals suggest the presence in solution of two additional tautomeric forms in equilibrium with the form characterized in the solid state. The tautomeric forms will be designated **IIa** (the single form in the solid state), **IIb**, and **IIc**.

(18) Haller, K. J.; Andersen, E. L.; Fehlner, T. P. *Inorg. Chem.* **1981**, *20*, 309.
(19) Wade, K. *Adv. Inorg. Chem. Radiochem.* **1976**, *18*, 1.
(20) Mingos, D. M. P.; Johnston, R. L. *Struct. Bonding* **1987**, *68*, 29.
(21) Calvert, R. B.; Shapley, J. R. *J. Am. Chem. Soc.* **1977**, *99*, 5225.
(22) Cowie, A. G.; Johnson, B. F. G.; Lewis, J.; Raithby, P. R. *J. Organomet. Chem.* **1986**, *306*, C63.
(23) Dutta, T. K.; Vites, J. V.; Jacobsen, G. B.; Fehlner, T. P. *Organometallics* **1987**, *6*, 842.

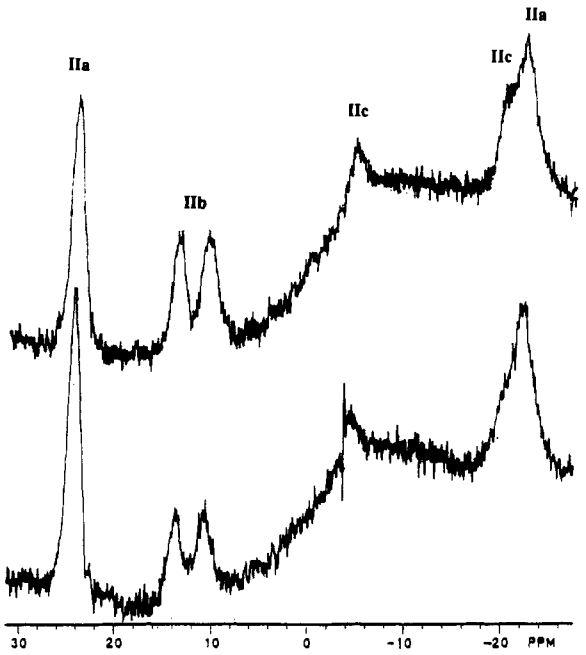

Figure 6. ^{11}B NMR spectra of crystals of **II** dissolved in toluene after 10–20 min (bottom) and after 40 min (top) showing the enhanced intensities of the resonances at δ 24 and −22 ppm. The broad powder signal is caused by boron in the NMR probe.

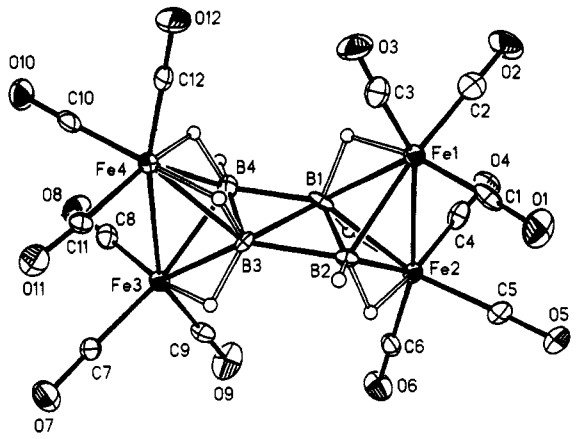

Figure 7. Molecular structure and labeling scheme for *B,B-conjuncto*-$[B_2H_4Fe_2(CO)_6]_2$ (**II**) in the solid state. The hydrogen atoms were located and refined. Atoms are shown as 50% thermal ellipsoids except for hydrogen atoms which are drawn at a fixed radius. Selected distances (Å) are as follows: Fe(1)–Fe(2) = 2.578(2), Fe(1)–B(1) = 2.088(9), Fe(1)–H(11) = 1.510(44), Fe(2)–B(1) = 2.193(10), Fe(2)–H(21) = 1.510(56), B(1)–B(2) = 1.714(13), B(1)–B(4) = 1.862(12), B(1)–H(21) = 1.271(67), B(2)–H(2) = 1.103(98), Fe(1)–B(2) = 2.139(9), Fe(2)–B(2) = 2.193(10), Fe(2)–H(22) = 1.514(66), B(1)–B(3) = 1.710(14), B(1)–H(11) 1.272(40), B(2)–B(3) = 1.907(11), B(2)–H(22) = 1.266(60).

On the basis of the integration of the ^{11}B NMR spectra, the ratio of abundances of these forms at 20°C is 6:3:1, respectively. An analogous situation has been observed in the case of C_4B_8 cages formed by the oxidative coupling of C_2B_4 cages.[24]

As we have been unable to crystallize either **IIb** or **IIc**, we had to rely on the spectroscopic measurements for characterization. Although there were changes in the IR spectrum of a sample of pure **II** as a function of temperature, they were relatively minor and the weak difference spectra could equally well be due to temperature effects other than changes in equilibrium ratios. Likewise the variable temperature (VT) ^{11}B NMR were uninformative in that at low temperature the quadrupolar broadening was excessive whereas at higher temperatures the production of I interfered. These experiments do suggest that the enthalpy differences between the tautomeric forms of **II** are very small.

All structural information on **IIb,c** has been derived from VT ^1H NMR experiments, and because of the low abundance of **IIc**, only a clear picture of **IIb** appears. The VT ^1H NMR spectra are summarized in Table I, and partial spectra are shown in Figure 8. Not only are tautomeric forms present (as described above) but processes rapid on the NMR time scale are taking place such that averaging of selected resonances can be seen. Thus, a unique assignment is not possible but the following is a reasonable one.

On the basis of the solid-state structure of **IIa** and the unambiguous ^1H NMR spectrum of **I**, the ^1H NMR resonances at −50°C due to **IIa** are assigned in a straightforward manner as follows. ^{11}B NMR for **IIa**: δ 24.2 (2 B), −21.9 (2 BH). ^1H NMR for **IIa** (−50°C): δ 3.0 ($2H_{term}$), −12.5 (2 BHFe), −12.7 (2BHFe), −16.4 (2BHFe). Note that the boron environment of the boron exhibiting the δ −21.9 resonance is similar to that of the boron atoms in $B_2H_6Fe_2(CO)_6$ (δ = −24.2) whereas the boron having no terminal proton is found at much lower field as expected.[25] Life becomes more complex at both higher and lower temperatures. At 65 °C the resonances at 3.0 and −16.4 coalesce at −6.6 (calcd −6.7). A simple mechanism, similar to that invoked to account for the fluxional behavior of $B_2H_6Fe_2(CO)_6$ and $[B_2H_5Fe_2(CO)_6]^-$,[14] is shown in Scheme I. Note that two ^{11}B resonances are observed at this temperature thereby eliminating other possibilities that would average the boron environments. The appearance of partially collapsed quartets emphasizes the coupling to boron and shows that the resonances at −11.5 and −12.7 have additional intensity due to other protons. The former is assigned to **IIc** while the latter is assigned to **IIb** by a process of elimination (see below). On the other hand, at -90 °C, the lowest temperature achieved, the clear changes taking place in the δ −12.7, -16.4, and 3.0 resonances suggests the freezing out of another exchange process. This suggests that the structure of **IIa** has lower symmetry than that shown by the solid-state structure determination.

The key to the assignment of **IIb** is the temperature independent resonances at δ −1.6, −11.5, and −14.7 of approximately equal intensities, which are due to BHB, BHFe, and BHFe protons, respectively (Table I). The intensity data as a function of temperature suggest that a third BHFe resonance lies at $\delta \approx$ −12.6. These intensities relative to those assigned to **IIa** are consistent with the assignment of the ^{11}B signals at δ 13.8 and 10.6 to **IIb**. The low-field shifts are consistent with the presence of no BH_{term} protons. The summary assignment then is as follows. ^{11}B NMR for **IIb**: δ 13.8 (2 B), 10.6 (2B). ^1H NMR for **IIb** (−50°C); δ −1.6 (2BHB), −11.5 (2 BHFe), −12.7 (2 BHFe), −14.7 (2 BHFe). One concludes that tautomer **IIb** is static over the temperature range examined, has two pairs of borons with no terminal hydrogens in similar environments, and has one pair of BHB and three pairs of BHFe bridging hydrogens. A structure consistent with these data is shown in Figure 9. Note that it is only the asymmetric distribution of *endo*-hydrogens that makes the pairs of boron atoms inequivalent. The relative intensities of the ^1H and ^{11}B NMR data for **IIa,b** show that at 20 °C **IIa** is more abundant than **IIb** whereas at 65°C they have nearly equal populations. Therefore the enthalpy of **IIa** is lower than that of **IIb**. Although not necessary, one tends to think of the most stable tautomer as the one most likely to crystallize out.

The data on the third tautomer is pretty thin. Although the ^{11}B NMR clearly reveals the presence of a third species, it is only at 65 °C that a clear indication of additional intensity evident in the ^1H NMR. This observation, and the VT ^{11}B spectra (Figure 5), suggest **IIc** has an even higher enthalpy than **IIb** and is only important at the higher temperatures. Two resonances that can be identified with BHFe protons can be assigned to **IIc** (Table I). The relative intensities suggests that there is another resonance (probably BH_{term}) that is not observed. A summary is as follows.

(24) Maxwell, W. M.; Miller, V. R.; Grimes, R. N. *Inorg. Chem.* **1976**, *15*, 1343.

(25) Rath, N. P.; Fehlner, T. P. *J. Am. Chem. Soc.* **1988**, *110*, 5345.

Table I. 500-MHz ^1H NMR Data for *B,B-conjuncto*-$[B_2H_4Fe_2(CO)_6]_2$ (II)

65 °C			20 °C			−50 °C			−90 °C		
δ	I^a	A^b	δ	I^a	A^b	δ	I^a	A^b	V	I^a	A^b
						3.0	2.0[c]	a	3.0	1.2[c]	a
									2.5	0.5[c]	a
−1.7	2.1	b	−1.7	1.1	b	−1.7	1.3	b	−1.7	1.2	b
−6.6	4.0	a	−6.6	2.9	a						
−11.6	2.7	b, 2.1 c, 0.6	−11.6	1.2	b	−11.5	0.9	b	−11.4	1.3	b
−12.6	6.3	a, 4.0 b, 2.3	−12.6	5.1	a, 4.0 b, 1.1	−12.6	2.8	a, 2.0 b, 0.8	−12.7	3.4	a, 2.0 b, 1.4
									−13.6	0.2	?
−14.6	3.3	b, 2.1 c, 1.2	−14.6	1.0	b	−14.7	1.0	b	−14.8	1.4	b
						−16.4	0.9	a	−16.2	0.7	a
									−16.6	1.3	a

[a] Relative area. [b] Assignment: a = IIa, b = IIb, c = IIc. [c] From −70 °C spectrum at 300 MHz.

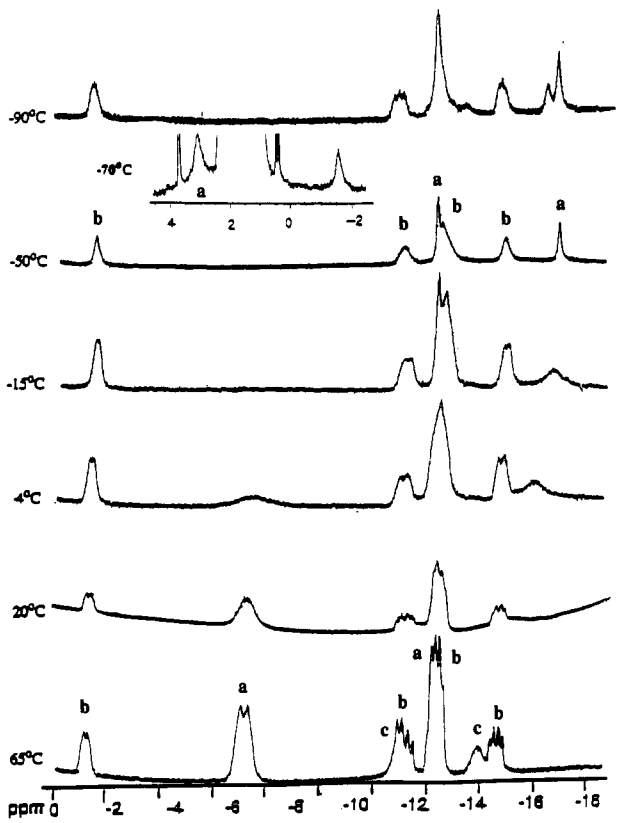

Figure 8. 500-MHz VT ^1H NMR spectra of *B,B-conjuncto*-$[B_2H_4Fe_2(CO)_6]_2$ (II) in toluene-d_8. The letters correspond to the assignments given in Table I and in the text. At low temperatures a resonance appears at δ 3.0 as shown in the inset.

Scheme I

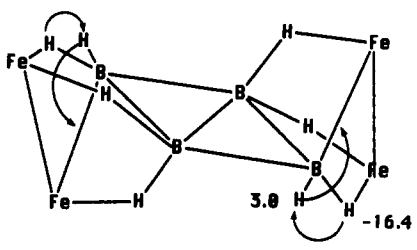

^{11}B NMR for IIc: δ −4.2 (2B), −20.0 (2BH). ^1H NMR for IIc (65 °C): δ BH_{term} not obsd, −11.4 (2BHFe), −14.0 (4 BHFe). The boron resonances are consistent with two types of boron atoms one of which is in an environment like that of $B_2H_6Fe_2(CO)_6$. A discussion of possible structures will be found below.

Definition of the Equilibrium Position. As shown in Figure 5 a pure sample of II when heated leads to a mixture of I and II, where the latter consists of an equilibrium mixture of three tautomers. Likewise, heating a sample of pure I leads to the identical equilibrium mixture at the same temperature. At 85°C the intensities of the resonances are independent of time. The ^{11}B NMR yields were nearly quantitative, and the isolated yields of the two isomers were also high. There must be a substantial energy barrier separating I and II as at 20 °C no sign of isomerization has been observed and the two geometric isomers can be separated by column chromatography. The equilibrium ratio, $K = [II]/[I]$, is equal to 2 at 85°C. Thus, the free energy difference is small; $\Delta G_o = -RT\ln K = -0.4$ kcal/mol. This should be contrasted with the tautomeric equilibria associated with II. Here small free energy differences and modest energy barriers separating the tautomeric structures are observed.

Thermolysis of $B_2H_6Fe_2(CO)_6$. In order to further confirm that low temperature oxidative coupling leads to a kinetic product, the products of the pyrolysis of $B_2H_6Fe_2(CO)_6$ were examined. On the basis of ^{11}B NMR spectroscopy, I and II are formed in the equilibrium ratio established above but are accompanied by a large amount of decomposition into other products. Thus, deprotonation followed by oxidative coupling constitutes a regiospecific pathway with a much better product yield.

Discussion

It is well-known that B–H–B and M–H–M bridging hydrogens are protonic in nature and can be removed by base to yield direct B–B and M–M bonds, respectively.[26,27] Likewise, B–H–Fe hydrogens can be removed as protons to yield B–Fe basic sites. In contrast to borane anions and related species,[26,28–31] the monoanions of ferraboranes are not sufficiently reactive to be useful as nucleophiles. Thus, for example, the monoanion, $[HFe_4(CO)_{12}BH]^-$, is unreactive toward CH_3I whereas the dianion, $[Fe_4(CO)_{12}BH]^{2-}$, reacts cleanly to yield $[HFe_4(CO)_{12}BCH_3]^-$.[32] It is not surprising then that it is only the dianion of $B_2H_6Fe_2(CO)_6$, $[B_2H_4Fe_2(CO)_6]^{2-}$, that undergoes the coupling reaction.

The observations suggest a stoichiometric mechanism similar to that proposed for the oxidative coupling of borane and carborane anions by Grimes and co-workers.[8] That is, a similar set of reagents has been used and these workers have demonstrated the presence of biscarborane Fe(II) and Co(III) intermediates. They have crystallographically characterized a trapped biscarborane

(26) Shore, S. G. In *Boron Hydride Chemistry*; Muetterties, E. L., Ed.; Academic Press: New York, 1975; p 79.
(27) *The Chemistry of Metal Cluster Complexes*; Shriver, D. F., Kaesz, H. D., Adams, R. D., Eds.; VCH: New York, 1990.
(28) Hawthorne, M. F. *J. Organomet. Chem.* **1975**, *100*, 97.
(29) Grimes, R. N. *Pure Appl. Chem.* **1982**, *54*, 43.
(30) Gaines, D. F. *Acc. Chem. Res.* **1973**, *6*, 416.
(31) Hosmane, N. S.; Maguire, J. A. In *Advances in Boron and the Boranes*; Liebman, J. F., Greenberg, A, Williams, R. E., Eds.; VCH: New York, 1988; p 297.
(32) Rath, N. P.; Fehlner, T. P. *J. Am. Chem. Soc.* **1987**, *109*, 5273.

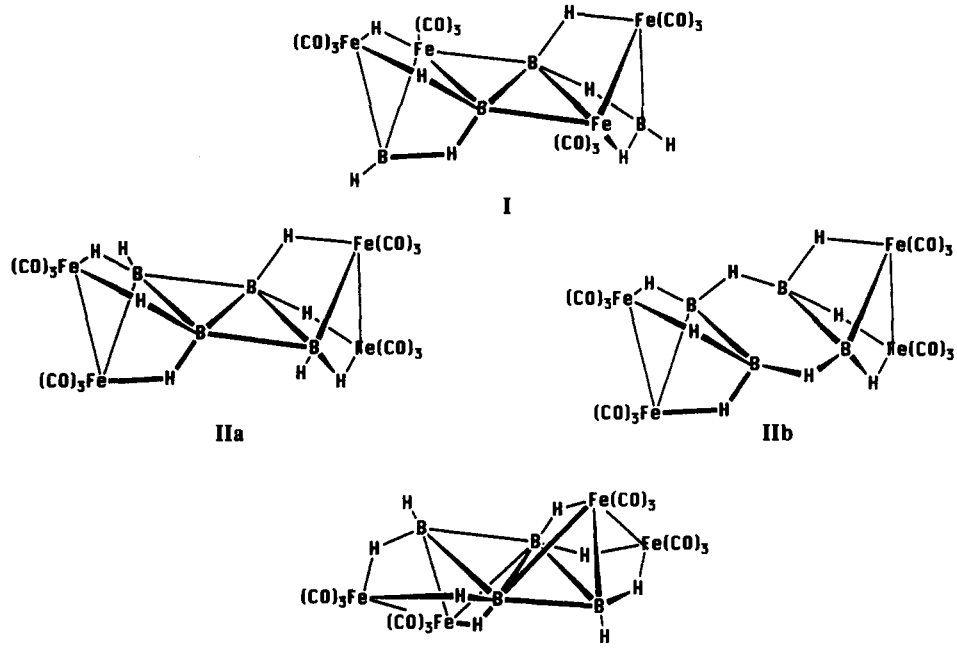

Figure 9. Structures of I and IIa–c. The first two are based on both solid-state X-ray diffraction and solution spectroscopic studies. The last two are proposed structures based on spectroscopic data only.

Chart II

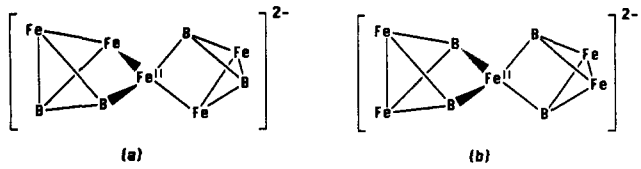

intermediate as well.[33] Although the experimental evidence here is neither as complete nor as conclusive, a similar pathway expressed by reactions 1 and 2 above is likely. Considering the intercage connectivity of the first product, I, an intermediate with the structure illustrated in Chart IIa rather than IIb is likely; i.e., it is an Fe–B rather than B–B edge bond of the dianion that coordinates to the Fe(II) center. The oxidation of this complex by 2 equiv of Fe(III) gives the kinetic product, *B,Fe-conjuncto*-$\{B_2H_4Fe_2(CO)_6\}_2$, I.

The first product, I, possesses some interesting features with respect to cluster bonding. It is a 76 polyhedral electron count (pec) E_4M_4 cluster molecule,[20] where E and M refer to main group and transition element atoms in the cluster core. The analogous M_8 cluster would have a 116 pec, but apparently there is only one example of such a cluster with a geometry consisting of two trigonal prisms sharing a square face.[34,35] On the other hand, $B_4H_4Ni_4Cp_4$ is a well known compound[36] that has a pec of 76 and a single cage dodecahedral geometry inconsistent with the electron counting rules.[37] Further, as we pointed out in our original communication, application of the counting rules for cluster coupling and fusion results in a pec of 74, i.e, two pec 40 E_2M_2 tetrahedral clusters fused in a transoid fashion to a pec 42 E_2M_2 butterfly cluster. These rules do not include the possibility of cluster–cluster coupling via three center–two electron bonds as is known for boranes.[38–42] Thus, the two B_2Fe_2 clusters of $\{B_2H_4Fe_2(CO)_6\}_2$ only have a pec of 38 rather than 40 and can be viewed as unsaturated clusters with an empty exo-cluster valence orbital centered on the boron atom with no terminal hydrogen atom (Scheme II). In an analogous fashion to BH_3, the unsaturated $B_2H_4Fe_2(CO)_6$ fragments dimerize via the formation of two closed three center–two electron B–Fe–B bonds. In contrast to BH_3, however, this dimerization does not appear to take place outside the coordination sphere of the iron atom of the postulated intermediate.

The major difference in the structures of I and II in the solid state (IIa) is the intercage connectivity by which the two B_2Fe_2 tetrahedra define B_2Fe_2 and B_4 diamond shapes, respectively (Figure 9). The electron counting is the same for both structures. This is easily appreciated by recalling the fact that the BH and $Fe(CO)_3$ fragments are isolobal; i.e., I and IIa differ only in the placement of a pair of BH and $Fe(CO)_3$ fragments. Alternatively, one can view I and II as containing a metal coordinated boron chain and a boron diamond shape, respectively. It is interesting to note in this regard that, in solid-state borides, the boron-rich systems are characterized by polyhedral boron networks (diamond motif) whereas the metal-rich systems exhibit isolated atoms, chains and sheets.[43] The similar energies of I and II suggest that the origin of such structural forms lies more in stoichiometry than energetics.

In contrast to I the characterization of II in solution is both complex and incomplete. However, certain points are clear. The predominate form of II in solution has the structure found in the solid state. Two other tautomeric forms exist in the solution state. The NMR data on the next most abundant tautomer suggest structure IIb (Figure 9). An isomerization analogous to IIa to IIb has been observed previously by Hawthorne and coworkers. The more stable tautomeric form of $[\{B_{10}H_9\}_2]^{2-}$ contains two ten boron cages joined by two closed three center–two electron

(33) Grimes, R. N.; Maynard, R. B.; Sinn, E.; Brewer, G. A. *J. Am. Chem. Soc.* **1982**, *104*, 5987.
(34) Arrigoni, A.; Ceriotti, A.; Della Pergola, R.; Longoni, G.; Manassero, M.; Masciocchi, N.; Sansoni, M. *Angew. Chem., Int. Ed. Engl.* **1984**, *23*, 322.
(35) Mingos, A. S.; Mingos, D. M. P. In *The Chemistry of Metal Cluster Complexes*; Shriver, D. F., Kaesz, H. D., Adams, R. D., Eds.; VCH: New York, 1990.
(36) Bowser, J. R.; Grimes, R. N. *J. Am. Chem. Soc.* **1978**, *100*, 4623.
(37) Cox, D. N.; Mingos, D. M. P.; Hoffmann, R. *J. Chem. Soc., Dalton Trans.* **1981**, 1788.
(38) Schwalbe, C. H.; Lipscomb, W. N. *Inorg. Chem.* **1971**, *10*, 151.
(39) Kaczmarczyk, A.; Dobrott, R. D.; Lipscomb, R. N. *Proc. Natl. Acad. Sci. U.S.A.* **1962**, *48*, 729.
(40) Pilling, R. L.; Hawthorne, M. F.; Pier, E. A. *J. Am. Chem. Soc.* **1964**, *86*, 3568.
(41) Chamberland, B. L.; Muetterties, E. L. *Inorg. Chem.* **1964**, *3*, 1450.
(42) Middaugh, R. L.; Farha, F. *J. Am. Chem. Soc.* **1966**, *88*, 4147.
(43) Thompson, R. In *Progress in Boron Chemistry*; Brotherton, R. J., Steinberg, H., Eds.; Pergamon: New York, 1970; Vol. 2.

Scheme II

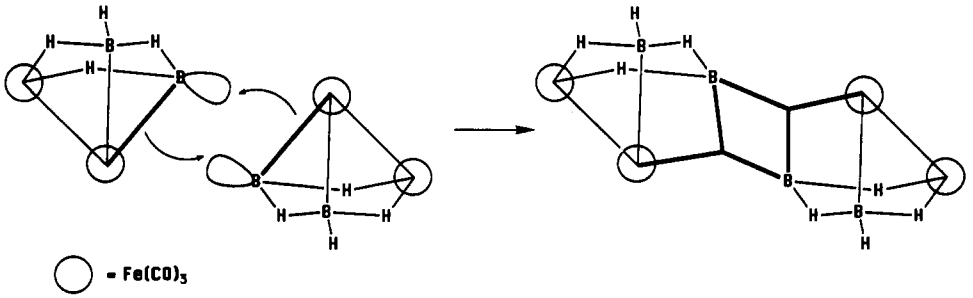

B–B–B bonds whereas in the other tautomer the two cages are joined by two three center–two electron BHB bonds.[40,44] Thus, in terms of bonding, the isomerization of **IIa** to **IIb** and that of $[\{B_{10}H_9\}_2]^{2-}$ involves the conversion of two B–H + B–B–B interactions into two B–H–B + B–B interactions. In contrast to the ferraborane system, photolysis is required to generate the latter which returns to the more stable form on heating at 100°C. This suggests that the barrier to rearrangement is larger in the main group cage than in the ferraborane, which implies that significant perturbation of the cluster itself must take place during the rearrangement process.

The least abundant form **IIc** is poorly characterized, but a couple of points are clear. First, like the other tautomers **IIc** possesses six BHFe protons in similar chemical environments and probably two BH_{term} protons. Second, the chemical environments of the two boron atom types are quite different suggesting a structure more like **IIa** than **IIb**. Third, any structure of **IIc** must be similar to that of the other tautomers in terms of the number and type of atom–atom interactions. Finally, the fact that **I** and **II** do not readily interconvert at 20°C suggests that the intercage connection still involves boron atoms. There are no model compounds in the literature; however, the electron counting rules provide additional possibilities even for coupled cages. An appealing possibility is a structure based on the B–B edge-fusion of two hypothetical 42 pec B_3Fe_2 trigonal bipyramidal clusters, e.g., 1,2-$B_3H_5Fe_2(CO)_6$, by the elimination of a B_2H_2 fragment to yield a 76 pec $B_4H_8Fe_4(CO)_{12}$ with the structure shown in Figure 9. Considering the more delocalized nature of the cluster electronic structure of a trigonal bipyramidal cluster compared to the electron precise tetrahedron, the difference between **IIc** and **IIa** or **IIb** lies in the extent of delocalized bonding. That is, an analysis in terms of two- and three-center bonding is less satisfactory. It is interesting to note that, although only two forms of $[\{B_{10}H_9\}_2]^{2-}$ have been characterized, the conversion of the (B–H–B + B–B) form to the (B–H + B–B–B) form is accompanied by the formation of a metastable intermediate.[44] One wonders if its structure is analogous to that of **IIc**.

Conclusions

The oxidative fusion reaction effectively used by Grimes and co-workers for the coupling of largely borane monoanions is also effective for at least one example of a metal-rich ferraborane. In the latter case it is necessary to use the dianion. The reaction conditions promote the formation of kinetic products which permits the study of cluster isomerization. The demonstration of four structural forms with nearly equal energies vividly demonstrates once again[23] the fact that for transition metal cluster systems numerous minima of similar energy exist on the potential energy surface. Hence, great care need be exercised in drawing general conclusions solely from solid state structures of a given cluster type.

Experimental Section

General Data. Reactions and manipulations were conducted under N_2 using standard Schlenk-line techniques. Glassware was oven- and flame-dried before use. Hexane, toluene, and tetrahydrofuran (THF) were predried by KOH and distilled from sodium/benzophenone ketyl under nitrogen. Diiron nonacarbonyl, $BH_3{\cdot}SMe_2$, *n*-butyllithium, $FeCl_2$, $FeCl_3$, and PPNCl (bis(triphenylphosphine)nitrogen(1^+) chloride) were used as received from Aldrich. $B_2H_6Fe_2(CO)_6$ was prepared by our published method.[45] Silica gel from Baker (60–200 mesh) was oven dried over night before use. Spectral data were obtained on the following instruments: ^1H, GE GN-300 or Varian-500 with shifts referenced to toluene-d_8 (δ 7.09); ^{11}B, Nicolet NT-300 with shifts referenced to $[B_3H_8]$-$[NEt_4]$ (δ −29.7); FT-IR, Nicolet 205. Mass measurements were obtained on a Finnigan-MAT 8430.

Preparation of $[B_2H_4Fe_2(CO)_6]Li_2$. A 185-mg sample (0.6 mmol) of yellow-orange $B_2H_6Fe_2(CO)_6$ was placed in a 40 mm diameter Schlenk tube under nitrogen as a hexane solution. After hexane was removed by vacuum distillation at −20 °C, the reaction tube was placed in a −78°C cold bath (dry-ice/acetone) and 25 mL of THF was added. A 0.6-mmol amount of *n*-butyllithium (0.4 mL of 1.6 M solution) was added drop by drop over a 10-min period, and the solution was stirred for an additional 10 min. Since the deprotonation reaction at −78 °C is very slow, the reaction tube was warmed to −20 °C. The solution immediately became intensely red indicating the formation of $[B_2H_5Fe_2(CO)_6]Li$ (Figure 1). ^{11}B NMR data showed quantitative conversion to the monoanion. The reaction tube was reintroduced to the −78 °C bath, 0.6 mmol of *n*-butyllithium was added drop by drop over a 1-h period, and then the solution was warmed to −20 °C. The IR data shows the formation of the dianion, but a large portion of the monoanion signals remains. The IR intensity of the dianion kept increasing during the addition of another 0.6 mmol of *n*-butyllithium. The color of the reaction mixture is deep reddish brown at this moment. Further addition of *n*-butyllithium results in destruction of the dianion. The dianion is extremely air-sensitive but stable as a lithium salt in THF at low temperatures. Fractional crystallization at −40 °C led to deep red crystals of the salt which are stable at low temperature but "melt" on warming. The relative intensities of the ^1H NMR signals suggests ≈2 THF molecules per Li atom in the salt. Removal of the THF causes the color of the material to change from red to brown. Unfortunately, we have been unable to obtain spectra free from the monoanion presumably because of the affinity of the dianion for protons; i.e., dissolution of the brown solid with fresh THF leads to a ≈2:1 mixture of the dianion:monoanion. The yield of $[B_2H_4Fe_2(CO)_6]Li_2$ from $B_2H_6Fe_2(CO)_6$ was estimated to be about 70% based on ^{11}B NMR data.

^{11}B-NMR (THF, 20 °C, δ): −20.6 (br, fwhm, 309 Hz, $\{^1H\}$ 230 Hz). ^1H-NMR (THF-d_8, 20 °C, δ): −5.2 (br, s, 4H); (THF-d_8, −30°C, δ) coalescence; (THF-d_8, −60 °C, δ) 1.2 (calcd, 2H), −11.6 (br, s, 2H); (THF-d_8, −90°C, δ) 2.4 (calcd, 2/3H), 0.6 (sh, 4/3H); −11.1 (br, s, 2/3H); −11.9 (br, s 4/3H). IR (THF, cm^{-1}): 2420 w (BH); 1965 m, 1940 (sh), 1904 vs, 1875 s, 1840 m,sh 1650 m (CO) (see also Figure 1).

Preparation of $B_4H_8Fe_4(CO)_{12}$, I. A 0.6-mmol amount of $[B_2H_4Fe_2(CO)_6]Li_2$ in 20 mL of THF solution was introduced into a 40 mm o.d.Schlenk tube. The reaction tube was placed in a −78 °C cold bath, and 77 mg of $FeCl_2$ (0.6 mmol) was added. The color of the solution changed from deep red to pale brownish yellow within 5 min. The solution was stirred for 1 h. The IR data showed that the dianion intensity had disappeared completely (Figure 2) and was replaced by new bands at higher frequency. Subsequently 195 mg of $FeCl_3$ (1.2 mmol) was added dropwise over the course of 1 h. Again there was a change in the solution color from brownish yellow to deep red. This was accompanied by changes in the IR spectrum (Figure 2). The solvent was removed by vacuum distillation and the products were extracted into toluene. The toluene was pumped away, and the products were introduced as a hexane solution

(44) Hawthorne, M. F.; Pilling, R. L. *J. Am. Chem. Soc.* **1966**, *88*, 3873.

(45) Meng, X.; Fehlner, T. P. *Inorg. Synth.* **1992**, *29*, 269.

on a silica gel column(1.6 × 12 cm, Kieselgel 60, EM Science). Degassed hexane was used as an eluent. At room temperature, four bands were observed with hexane elution. The first band was unreacted $B_2H_6Fe_2(CO)_6$ monomer. The second band (red-orange) was collected as $B_4H_8Fe_4(CO)_{12}$ isomer I (R_f = 0.45). The product for spectroscopic analysis was dried under vacuum and gave 80 mg of pure material corresponding to a yield of 43% based on $[B_2H_4Fe_2(CO)_6]Li_2$. Reddish-orange crystals were grown in hexane solution by the slow cooling method from room temperature to −20 °C overnight. These were used for the X-ray structural analysis. The crystals are air sensitive and highly soluble in all organic solvents. The third band was a known ferraborane, $Fe_4(CO)_{12}BH_2$, and the fourth band is now identified to be $B_4H_8Fe_4(CO)_{12}$ isomer II. The initial formation yield of $B_4H_8Fe_4(CO)_{12}$ isomer II is estimated to be about 4% based on ^{11}B-NMR intensities. However, $B_4H_8Fe_4(CO)_{12}$ isomer II has a tendency to stick on silica gel (Kieselgel 60) and the existence of $B_4H_8Fe_4(CO)_{12}$ isomer II only became clear when the isomerization reaction of I was carried out.

^{11}B-NMR (hexane, 20 °C, δ): 0.8 (br, fwhm, 102 Hz, {^{1}H} 69 Hz), −2.5 br, d, J_{BH} = 117 Hz).^{1}H NMR (C_6D_6, 20°C, δ): 3.1 (br, 2H), −1.2 (br, 2H), −13.0 (br, 2H), −14.6 (br, 2H). IR (hexane, cm^{-1}): 2524 vw (BH); 2088 w, 2067 m, 2034 vs, 2018 w, 2003 m, 1983 w (CO). MS (EI, *m/e*): P^+ = 612 (−12 CO); $^{56}Fe_4{}^{12}C_{12}{}^{16}O_{12}{}^{11}B_4{}^1H_8{}^+$, 611.7776 obsd, 611.7799 calcd. The details of the X-ray structure determination have been reported previously.[13]

The deprotonation of I with 1 equiv of BuLi followed by methathesis with PPNCl led to the monoanion. IR (Et_2O, cm^{-1}): 2491 vw (BH); 2067 m, 2024 s, 2014 s, 2005 s, 1988 m, 1977 s, 1950 m, 1938 sh (CO). The deprotonation of I with 2 equiv of BuLi followed by methathesis with PPNCl led to the dianion. IR (Et_2O, cm^{-1}): 2475 vw (BH); 2024 w, 1992 s, 1981 m, 1965 vs, 1938 s, 1920 sh (CO).

Preparation of $B_4H_8Fe_4(CO)_{12}$, II. A 61-mg amount (0.1 mmol) of $B_4H_8Fe_4(CO)_{12}$ isomer I was placed in a 20 mm o.d. Schlenk tube, and 10 mL of toluene was added. The reaction tube was dipped into an oil bath (90°C) and stirred. The initial reddish-orange color gradually changed to deep red. After 1 h, the ^{11}B NMR spectrum showed that 70% of isomer I was converted to isomer II. However, the remaining isomer I signal did not diminish even after 4 h at higher temperatures (100–115 °C). After removal of the toluene, the reaction mixture was loaded on a silica gel column (1.6 × 12 cm, Baker, 60–200 mesh) as a hexane solution. With hexane elution, two bands were separated. The first reddish-orange band was unconverted isomer I, and the second red band (R_f = 0.3) was identified as isomer II. Deep red crystals formed in toluene solution by slow cooling (20 to −10 °C) over a 2-day period. The crystals are moderately air sensitive and poorly soluble in nonpolar organic solvents. The isolated yield was 62% (38 mg). Isomer II tends to stick on the silica gel column whereas isomer I does not.

^{11}B-NMR (THF, 20°C, δ): 24.25 (br, fwhm, 192 Hz, {^{1}H} 170 Hz, *I* = 0.6), 13.78 (br, fwhm, 220 Hz, {^{1}H} 190 Hz, *I* = 0.3), 10.56 (br, fwhm, 210 Hz, {^{1}H} 180 Hz, *I* = 0.3), −4.2 (br, fwhm, 220 Hz, {^{1}H}, 180 Hz, *I* = 0.1), −19.99 (sh) and -21.93 (br, fwhm, 270 Hz, {^{1}H}, 190 Hz, *I* = 0.7). ^{1}H-NMR: see Table I and Figure 5. IR (hexane, cm^{-1}): 2516 vw (BH); 2095 vw, 2074 s, 2059 w, 2046 vs, 2039 s, 2028 m, 2012 w, 1994 w, 1986 w (CO), MS(EI, *m/e*): P^+= $^{56}Fe_4{}^{12}C_{12}{}^{16}O_{12}{}^{11}B_4{}^1H_8{}^+$, 611.7808 obsd, 611.7799 calcd.

X-ray Structure Determination of $B_4H_8Fe_4(CO)_{12}$, II. An opaque dark red prism of II, 0.2 x 0.5 x 0.5 mm, was placed in an oil and mounted on the end of a glass fiber. Data were collected on a Siemens P3 diffractometer using graphite-monochromated Mo Kα radiation and equipped with a University of Wisconsin modified Siemens LT device. Cell parameters were determined from 14 peaks with $27 \le 2\theta \le 29°$. The space group $P2_1$ was determined by the systematic absences and intensity statistics and confirmed by refinement of the structure. Intensity data were collected in the ranges $3 \le 2\theta \le 50°$, (±h,±k,+l). Data were collected using the θ–2θ scan mode with a 2θ scan range of 2° + Kα separation and a variable scan speed of 2–20°/min. Three monitor peaks were remeasured with every 100 data and had a maximum variation of 0.08. An absorption correction was applied using the program XABS.[46] No extinction correction was applied. The 3744 intensities collected merged to 3613 independent data (R_{int} = 0.0473) yielding 3458 observed ($I > 2\sigma(I)$) intensities. The structure was solved by direct methods. Hydrogen positions were determined from a difference map and refined independently. Non-hydrogen atoms were refined using anisotropic thermal parameters. The refinement converged to $R(F) = 0.0568$, $R_w(F) = 0.0708$, and $S = 1.88$ using 316 variables and a weighting scheme of $w^{-1} = \sigma^2(F) + 0.0009F^2$. The largest $\Delta/\sigma = +0.023$; the range of difference map densities was $1.24 \le \rho \le -1.22$ e Å^{-3}. The difference map peaks with $\rho > 0.8$ e Å^{-3} were about 1 Å from the metals. Structure solution and refinement [minimizing $\Sigma w(F_o - F_c)^2$] was carried out using the SHELXTL PLUS program system[47] on a Micro VAX II computer. Other data collection and refinement details are listed in Table II.

Table II. Crystallographic Data for *B,B-conjuncto*-$[B_2H_4Fe_2(CO)_6]_2$ (II)

$B_4H_8Fe_4C_{12}O_{12}$	fw 610.8
a = 7.3740(10) Å	monoclinic $P2_1$
b = 13.956(3) Å	λ = 0.710 73 Å
c = 10.627(2) Å	d(calcd) = 1.932 g/cm^3
β = 106.22(3) deg	μ = 2.766 mm^{-1}
V = 1050.1(3) Å^3	$R(F)^a$ = 0.0568
Z = 2	$R_w(F)^a$ = 0.0708
T = −160(2) °C	S = 1.88

^{a} $R(F) = \Sigma(||F_o| - |F_c||)^2/\Sigma(|F_o|)^2$; $R_w(F) = [\Sigma(F_o - F_c)^2/\Sigma w(F_o)^2]^{1/2}$.

Preparation of *B,Fe-conjuncto*-$B_4H_8Fe_4(CO)_{12}$, I, from *B,B-conjuncto*-$B_4H_8Fe_4(CO)_{12}$, II. A31-mg amount (0.05 mmol) of $B_4H_8Fe_4(CO)_{12}$ isomer II was dissolved in 2 mL of toluene and introduced into a 10-mm NMR tube. The ^{11}B NMR signals were monitored as the sample was heated from room temperature to 85 °C. ^{11}B-NMR data show that isomer I forms at 85°C (30% of the total ^{11}B signal intensity). The sample was cooled back to room temperature and loaded on a silica gel column (1.6 × 12 cm, Baker) as a hexane solution after toluene was removed. With hexane elution, two bands were separated. The first reddish-orange band was identified as $B_4H_8Fe_4(CO)_{12}$ isomer I (8.3 mg, elution time, 90 min), and the second red band as $B_4H_8Fe_4(CO)_{12}$ isomer II (15.1 mg, elution time, 105 min).

^{11}B-NMR Spectra of *B,B-conjuncto*-$B_4H_8Fe_4(CO)_{12}$, II, as a Function of Time in Toluene Solution. After the isomer II was isolated from a silica gel column, slow removal of toluene resulted in the formation of microcrystals. The solids were washed with cold (0°C) hexane and dried under vacuum. The 2 mL of toluene extract of these solids was transferred into a 10-mm NMR tube. The first ^{11}B NMR measurement was performed 5 min after the crystals were dissolved. The ^{11}B signals were collected for about 5 min. The second data collection was done after 40 min had elapsed.

Thermolysis of $B_2H_6Fe_2(CO)_6$. A1.0-mmol amount (310 mg) of $B_2H_6Fe_2(CO)_6$ in 5 mL of toluene was placed in a 20 mm o.d. Schlenk tube. The reaction tube was dipped into a 90 °C oil bath. The orange color gradually changed to red after a couple of hours and then to reddish brown after several more hours. The progress of the reaction was monitored by ^{11}B NMR, and the signal of $B_2H_6Fe_2(CO)_6$ decreased very slowly. After 20 h, the reaction tube was removed from the oil bath and the toluene removed under vacuum. The products were loaded on a silica gel (1.6 × 12 cm, Baker) column as a hexane solution. Four major bands were observed. The first band was unreacted $B_2H_6Fe_2(CO)_6$, the second band was $B_4H_8Fe_4(CO)_{12}$ isomer I, the third band was a mixture among which one product exhibits the ^{11}B resonance of $HFe_4(CO)_{12}BH_2$, and the fourth band was $B_4H_8Fe_4(CO)_{12}$ isomer II. The second and the third bands are not separated cleanly with the Baker silica gel. The isolated yield of $B_4H_8Fe_4(CO)_{12}$ isomer II was 6% (18 mg). The optimized reaction time is 16–20 h at 90°C.

Acknowledgment. The support of the National Science Foundation is gratefully acknowledged. We thank Mr. Donald Schifferl for his aid with the NMR experiments and Dr. Xiangsheng Meng for his contributions to the synthesis of the dianion of $B_2H_6Fe_2(CO)_6$.

Supplementary Material Available: A packing diagram and tables of atomic positional and equivalent isotropic displacement parameters, selected bond distances and bond angles, anisotropic displacement coefficients, and H-atom coordinates for II (6 pages). Ordering information is given on any current masthead page.

(46) Hope, H.; Moezzi, B. Program XABS. The program obtains an absorption tensor from $F_o - F_c$ differences: Moezzi, B. Ph.D. Thesis, University of California, Davis, 1987.

(47) Sheldrick, G. M. SHELXTL PLUS version 4.2, Siemens Analytical X-ray Instruments: Madison, WI, 1990.